

DOI: 10.1002/anie.200502172

Kinetics and Mechanism of the Electrooxidation of Formic Acid—Spectroelectrochemical Studies in a Flow Cell***Yan Xia Chen,* Martin Heinen, Zenonas Jusys, and Rolf Jürgen Behm**

The application of in situ infrared spectroscopy in electrochemistry is well established. It has been particularly useful in electrocatalytic studies, in which the knowledge of the adsorbed species can contribute significantly to a fundamental understanding of the reaction mechanism (see, for example, reviews [1–3] and references therein). Most of these studies were conducted by using IR reflection absorption spectroscopy (IRRAS) techniques in a thin-layer configuration, where the thickness of the electrolyte layer between the electrode and the IR window is limited to about 10 μm to keep spectral contributions from the electrolyte at a tolerable level. Under these conditions mass transport in the thin-layer gap is practically inhibited, which may result in strongly misleading conclusions on the reaction process owing to the depletion of reactants as well as accumulation and possibly readsorption of by-products.^[2]

These limitations can be reduced by performing infrared absorption reflection spectroscopy measurements in an attenuated total reflection configuration (ATR-FTIRS),^[4,5] in which a thin metal film deposited on an optical prism serves as a working electrode and the IR beam is transmitted internally from the back side of the prism to the film and totally reflected at the prism/film interface. In this technique the working electrode is freely accessible to the electrolyte. Nevertheless, despite the obvious improvements over the thin-layer configuration, diffusion of reactants to and products from the electrode is still ill-defined.

Herein we describe an extension of the present in situ ATR-FTIRS technique by coupling it to a thin-layer electrochemical flow cell. We demonstrate the potential of this technique for mechanistic and kinetic studies of electro-

[*] Dr. Y. X. Chen, M. Heinen, Dr. Z. Jusys, Prof. Dr. R. J. Behm
Dept. Surface Chemistry and Catalysis
University of Ulm
89069 Ulm (Germany)
Fax: (+49) 731-502-5452
E-mail: yan-xia.chen@uni-ulm.de
juergen.behm@uni-ulm.de

[**] We gratefully acknowledge the help of M. Osawa and S. Ye (University of Hokkaido, Japan) in introducing the ATR-FTIRS technique as well as financial support by the Forschungsallianz Brennstoffzellen (FABZ) Baden-Württemberg and by the Deutsche Forschungsgemeinschaft (BE 1201/8-4, BE 1201/11-1). Y.X.C. is grateful for a fellowship from the Alexander von Humboldt Foundation.



Supporting information for this article is available on the WWW under <http://www.angewandte.org> or from the author.

catalytic reactions, with the electrooxidation of formic acid on a Pt film electrode as an example. This reaction can be considered as a model reaction for the electrooxidation of small organic molecules. In addition, it is also of technical interest, as formic acid is a reaction intermediate in direct methanol fuel cells^[6] and was also proposed as a fuel for low-temperature fuel cells.^[7] It is generally accepted that the reaction proceeds through two different reaction pathways (“dual-path mechanism”): an “indirect” pathway involving formic acid dehydrogenation and subsequent electrooxidation of the resulting adsorbed CO to CO₂, and a “direct” pathway, which proceeds directly, without CO_{ad} formation, to CO₂.^[3,8,9] Recently, adsorbed formate was suggested as a stable intermediate.^[10] Our data demonstrate that this picture is incomplete and that the reaction involves at least three different parallel reaction pathways. The relative contributions of the three pathways under current reaction conditions are estimated from the electrochemical and IR spectroscopic data.

This study demonstrates the general potential of in situ ATR-FTIRS studies under continuous flow conditions with well-defined mass transport to/from the electrode, which is particularly important for reaction studies involving dissolved gases or other dilute reactants. Among others, this technique allows:

1. transient, time-resolved spectroelectrochemical measurements upon sudden exchange of the electrolyte under potential control;
2. spectroelectrochemical adsorption/stripping measurements of nonvolatile species;
3. modification of electrode surfaces by chemical or electrochemical adsorption/deposition in the flow cell prior to the actual measurements, which opens the way for a direct comparison of different surfaces.

Thus, this technique is of general relevance for kinetic and mechanistic spectroelectrochemical studies, by far exceeding applications in electrocatalysis.

The thin-layer spectroelectrochemical flow cell used in this study is analogous to that of a dual thin-layer flow cell design introduced recently,^[11,12] which was modified for the present measurements. It consists of a circular Kel-F plate with openings for inlet and outlet capillaries, counter- and reference electrodes, and a hemicylindrical silicon prism, which is pressed against the Kel-F plate through a circular gasket and a Cu foil current collector (Kel-F = poly(chlorotrifluoroethylene)). A thin Pt film deposited on the flat reflecting side of the Si prism serves as the working electrode.^[5] The electrolyte flow through the cell can be switched between different electrolytes.

The interaction of formic acid with Pt electrodes at potentials below oxide formation leads to the build-up of an adsorbate layer, whose chemical nature/composition depends critically on the electrode potential.^[9] The accumulation of the adsorbed species was monitored in potentiostatic, transient experiments under continuous electrolyte flow, changing from pure base electrolyte (0.5 M H₂SO₄) to formic acid containing electrolyte (0.5 M H₂SO₄ + 0.1 M HCOOH, *t* = 0–4.5 min); after reaching steady-state conditions (*t* = 4.5 min),

the current electrolyte was changed back to pure base electrolyte (adsorption/oxidation potential 0.4, 0.5, and 0.6). The nature of the adsorbed species is evident from the sequence of IR spectra in Figure 1, which were taken during

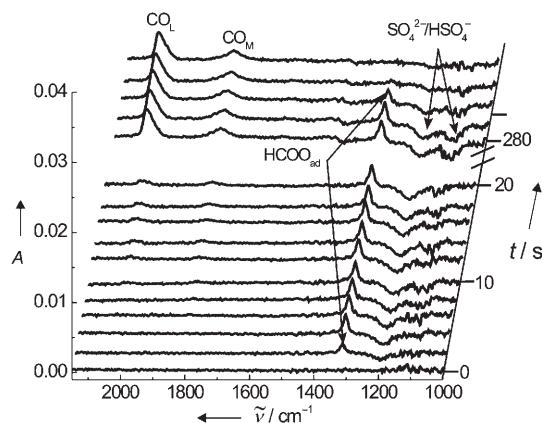


Figure 1. Selected IR spectra recorded during adsorption/oxidation of formic acid on a Pt thin film electrode at 0.5 V. Electrolyte exchange at *t* = 0 s from 0.5 M H₂SO₄ to 0.1 M HCOOH + 0.5 M H₂SO₄ and back after ≈ 4.5 min (270 s). Electrolyte flow rate: 50 μL s⁻¹, cell volume: 10–20 μL.

these transient experiments at a constant potential of 0.5 V. Characteristic features of these spectra are three positive bands, one with a signal at $\tilde{\nu} \approx 1322 \text{ cm}^{-1}$, which was attributed to bridge-bonded adsorbed formate (HCOO_{ad}),^[10,13] and two peaks centered at $\tilde{\nu} \approx 2010$ and 1790 cm^{-1} , which are related to linearly bonded (CO_L) and multiply bonded (CO_M) adsorbed CO (CO_{ad}). In addition, the spectra exhibit a two negative bands in the region $\tilde{\nu} = 1000\text{--}1250 \text{ cm}^{-1}$, which correspond to displaced bisulfate and sulfate.^[2] The presence of significant amounts of other adsorbates can be excluded based on the IR data. Spectra taken at 0.4 and 0.6 V exhibit similar characteristics as those above.

More quantitative information on the build-up of the adsorbate layer and on the relationship between adsorbate coverage and the Faraday reaction current is derived from the current densities in the chronoamperometric transients (Figure 2a) and from the integrated intensities of the IR signals as a function of time at the different adsorption potentials (Figures 2b–d). The current densities increase steeply when switching from the supporting electrolyte to HCOOH-containing solution (*t* = 0), reaching a maximum after approximately 3 s, and then decrease slowly with time under a continuous flow of HCOOH-containing electrolyte. When changing back to pure supporting electrolyte after about 4.5 min, they instantaneously drop to 0.

In contrast to the steep increase of the current densities, the intensities of the signals for adsorbed CO_L (Figure 2b) and CO_M (Figure 2c) develop slowly upon changing to 0.1 M HCOOH containing solution over the entire adsorption time (4.5 min). Both the final CO_{ad} coverage and the initial rate for CO_{ad} formation are highest for adsorption at 0.4 V, lower at 0.5 V, and very low at 0.6 V. When the electrolyte is switched

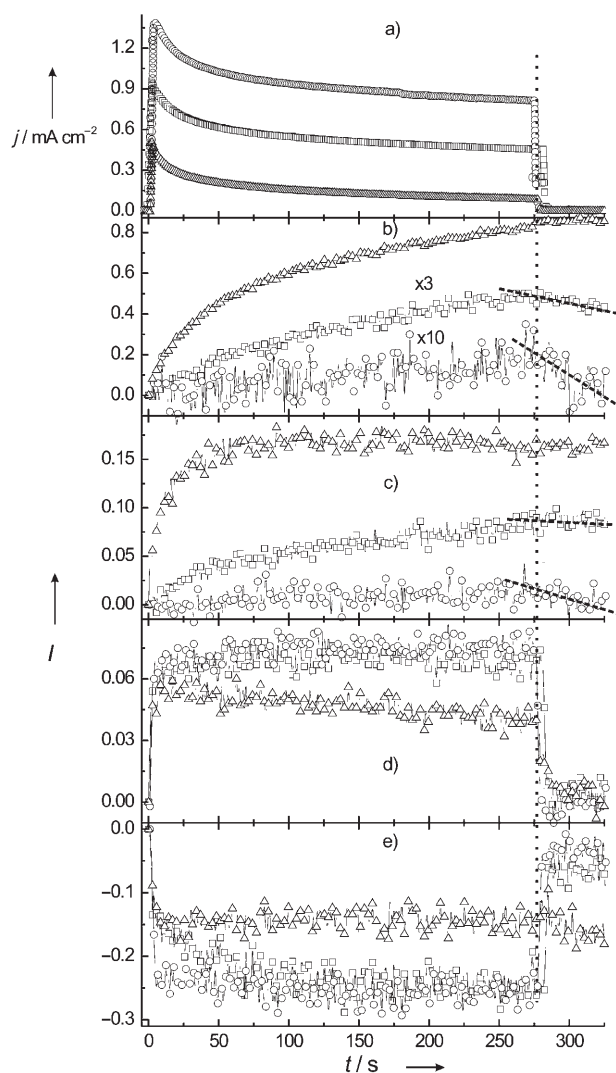


Figure 2. Chronoamperometric transients (a) and evolution of the IR peak intensities related to adsorbed CO_L (b) and CO_M species (c) as well as to adsorbed formate (d) and bisulfate and sulphate (e) during the interaction of formic acid with the Pt thin film electrode at 0.4 (Δ), 0.5 (\square) and 0.6 V (\circ) (experimental conditions see Figure 1).

back to HCOOH -free solution, the intensities of the CO_{ad} signals (Figure 2b) decrease only slowly, as expected from the slow kinetics of CO_{ad} electrooxidation at potentials of 0.6 V and below. The HCOO_{ad} -related intensities (Figure 2d) show an abrupt increase when switching to HCOOH -containing solution and reach an approximately constant value approximately 3 s after the electrolyte exchange. For adsorption at 0.4 V we find a slight subsequent decay of the formate band intensity with time, probably owing to formate replacement by CO_{ad} . Formate formation is accompanied by a decrease in the bisulfate and sulfate band intensity (Figure 2e), which approximately mirrors the temporal evolution of the formate intensity (Figure 2d), implying that sulfate/hydrogen sulfate is displaced by more strongly adsorbed formate species.

Similar to the current density, the formate intensity drops instantaneously to 0 when changing back to pure supporting electrolyte, accompanied by a similarly fast increase in the

bisulfate and sulfate intensity. Only at 0.4 V does the bisulfate and sulfate intensity remain virtually constant, despite the abrupt decay in formate intensity. This is tentatively explained by a combination of two effects: We expect that formate is randomly distributed in the CO_{ad} layer and that at the high CO_{ad} coverage a relaxation of the CO_{ad} layer is energetically more feasible than adsorption of the large and weakly adsorbed sulfate anions.

The above results clearly show that oxidation of formic acid is accompanied by the formation of adsorbed formate, in agreement with findings in a previous study,^[10] and that under the present reaction conditions the build-up of these formate species is much faster than the formation of CO_{ad} . Hence, the rate of formic acid dehydrogenation/ HCOO_{ad} formation (in this term we also include contributions from adsorption of formate anions from the electrolyte) is much higher than that for formic acid dehydration (CO_{ad} formation) under the present reaction conditions.

The reaction rates for the dehydration of formic acid to CO_{ad} and subsequent oxidation of CO_{ad} can be determined quantitatively from the IR data by using the relationship between the CO_{ad} coverage and the IR intensities for the CO_M species at low CO_{ad} coverages and the CO_L -related intensity in the medium CO_{ad} -coverage regime, which were determined in calibration measurements (see Supporting Information). The CO_{ad} oxidation rate under steady-state conditions is determined from the initial slope of the CO_{ad} intensity–time curve, right after changing back from a HCOOH -containing solution (1M) to HCOOH -free electrolyte (Figure 2b), assuming that the CO_L/CO_M population ratios do not vary significantly between 0.4 and 0.6 V.^[14] For clarity, we magnified the intensities of the CO_L species at 0.5 V (squares) by a factor of 3 and at 0.6 V (circles) by a factor of 10. We used a saturation coverage of 0.7 monolayers (ML) to calculate turnover frequencies (TOFs) of 6.4×10^{-5} and 3.3×10^{-4} molecules per Pt site per second for CO_{ad} oxidation to CO_2 at 0.5 and 0.6 V, respectively, under the present steady-state reaction conditions. At 0.4 V the rate for CO_{ad} oxidation is below our detection limit (Table 1). The increase in CO_{ad} oxidation rate with potential agrees with the common explanation of enhanced OH_{ad} formation at higher potentials (“electrochemical activation”).

In the same way we can determine the initial rates for CO_{ad} formation (HCOOH dehydration) on the initial, CO_{ad} - and HCOO_{ad} -free Pt surface from the initial slopes of the CO_{ad} intensity profiles, after switching from base electrolyte

Table 1: Turnover frequencies (TOF).^[a]

| Reaction | TOF [molecules s^{-1} site $^{-1}$] | | |
|---|---|----------------------|----------------------|
| | 0.4 V | 0.5 V | 0.6 V |
| HCOOH dehydration ^[b] | 2.0×10^{-2} | 1.8×10^{-3} | 3.2×10^{-4} |
| CO_{ad} oxidation ^[c] | ≈ 0 | 6.4×10^{-5} | 3.3×10^{-4} |
| total HCOOH oxidation ^[d] | 0.3 | 1.4 | 2.5 |

[a] TOF for [b] formic acid dehydration to CO_{ad} on a clean Pt surface (in the limit of very small CO_{ad} and OH_{ad} coverages), [c] CO_{ad} oxidation to CO_2 (steady state), [d] total oxidation of formic acid to CO_2 under steady state conditions, determined after 4.5 min under continuous flow of 0.1 M HCOOH + 0.5 M H_2SO_4 at different reaction potentials.

to HCOOH-containing solution. This yields values of 2.0×10^{-2} , 1.8×10^{-3} , and 3.2×10^{-4} molecules per Pt site per second for turnover frequencies of 0.4, 0.5, and 0.6 V, respectively (Table 1).

In the later stages of the adsorption process the increase in CO_{ad} coverage represents the difference between CO_{ad} formation (formic acid dehydration) and CO_{ad} oxidation; under steady-state conditions the two rates are equal. At 0.6 V the rates for CO_{ad} oxidation (on a partly CO_{ad} -covered Pt surface) and formic acid dehydration (on a bare Pt surface) are of comparable magnitude, which explains the rather low steady-state CO_{ad} coverage detected at this potential. At 0.4 V the CO_{ad} oxidation rate is negligible, resulting in the observed pronounced accumulation of CO_{ad} with time up to saturation. The absolute values of the initial dehydration rates as well as the fact that at 0.4 V the initial rate for formic acid dehydration is about (more than) one order of magnitude higher than at 0.5 V (0.6 V) agree well with results derived by Sun from electrochemical transients.^[3]

The relative contribution of the indirect reaction pathway to the total rate of oxidation of formic acid to CO_2 under the present steady-state conditions can be calculated from the ratio of the rate for oxidation of CO_{ad} determined above and the Faraday current under these conditions by using the values obtained from the chronoamperometric transients (Figure 2a) after oxidation of formic acid for 4.5 min (Table 1). Comparing the TOFs of 0.28, 1.4, and 2.5 molecules per Pt site per second for the oxidation of formic acid to CO_2 at potentials of 0.4, 0.5, and 0.6 V, respectively, and the above turnover frequencies for CO_{ad} oxidation at these potentials, we conclude that the indirect pathway, through dehydration of a HCOOH_{ad} precursor to CO_{ad} and its further oxidation to CO_2 , contributes less than 0.1% to the total rate of the oxidation of formic acid at 0.5 V and less than 0.01% at 0.6 V.

Interestingly, the ratio of the formate band intensities at the end of the HCOOH oxidation period at different potentials (Figure 2d) differs significantly from that of the Faradaic currents (Figure 2a): 90% (0.5 V) and 50% (0.4 V) of the formate intensity at 0.6 V result in Faradaic currents of 55% (0.5 V) and $\approx 10\%$ (0.4 V) of the value at 0.6 V, respectively. Since the dehydration pathway does not contribute significantly under these conditions, this observation requires either a potential-dependent variation (electrochemical activation) of both adsorbed formate formation and its oxidation to CO_2 , or the existence of another, third reaction pathway. For more information on this point we performed similar transient oxidation measurements as in Figure 2 at the same potential (0.6 V), using two different formic acid concentrations.

Representative results are shown in Figure 3. Comparing the Faraday currents for the oxidation of 0.7 mM and 70 mM HCOOH solution at 0.6 V, we find current densities of 0.045 mA cm^{-2} and 0.85 mA cm^{-2} , respectively, after 100 s, that is, roughly a factor of 20 between the two electrolytes. The IR spectra acquired at $t = 100 \text{ s}$, in contrast, show that the respective formate intensities differ only by about a factor of 5. Hence, even at similar reaction potential the total steady-state rates for HCOOH oxidation are not at all proportional to the respective formate coverages. Based on the negligible

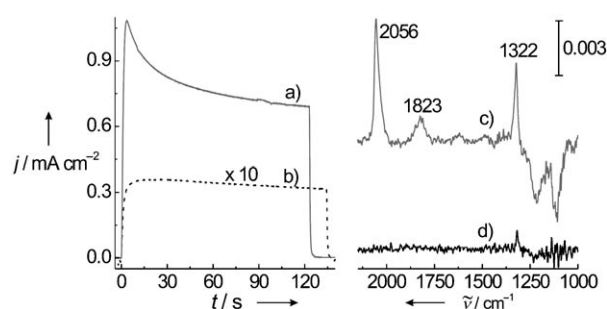


Figure 3. Chronoamperometric transients (a, b) and IR spectra of adsorbed formate (c, d) on a Pt thin film electrode at 0.6 V in a solution containing 70 mM (a, c) and 0.7 mM HCOOH (b, d). The spectra were acquired 100 s after changing to HCOOH-containing solution.

contribution of the indirect pathway under these conditions and assuming that the rate of formate decomposition is related linearly to formate coverage, these data clearly indicate that there must be a third reaction pathway.

Its contribution to the total reaction rate cannot be calculated precisely from these data, but we can estimate a higher limit for its contribution. Assuming that for 0.7 mM HCOOH solution the Faraday current results completely from the formate pathway, the fivefold-higher formate-band intensity in 70 mM HCOOH solution should at most result in a fivefold-higher current density. The experimentally observed increase by a factor of 20 is only possible if the reaction pathway via the adsorbed formate species detected by IR and dominating the formate IR signal (“formate pathway”) contributes less than 25% to the total anodic current.

Although our IR spectra do not give any indication of another adsorbed species, this third pathway is dominant for room-temperature oxidation of a 0.1 M formic acid solution. This can either be explained by an additional, thus far not detected adsorbed reaction intermediate, whose concentration is very low (low lifetime under reaction conditions), or by a direct reaction of weakly adsorbed HCOOH_{ad} species. (The theoretical possibility of a flat-lying formate species with a very low IR cross-section is ruled out as considerable substrate–adsorbate bonding would be necessary for a stable reaction intermediate.)

We favor the latter explanation and propose a triple path mechanism; which starts with a weakly adsorbed HCOOH_{ad} precursor that can subsequently either be directly oxidized to CO_2 (direct pathway), undergo dehydration to CO_{ad} (“indirect pathway”), or is dehydrogenated to stable bridge-bonded adsorbed formates (formate pathway), as it is schematically depicted in Figure 4. The stable, adsorbed intermediates resulting in the last two pathways can then, in a third step, be oxidized to CO_2 . In this scheme adsorbed formates are indeed reaction intermediates, but, in contrast to recent concepts,^[13] are not in the dominant reaction pathway.

In summary, we have 1) significantly improved the capability of in situ ATR-FTIRS measurements by combining this technique with a thin-layer flow cell, which allows mechanistic and quantitative spectroelectrochemical kinetic studies of electrocatalytic reactions under well-defined mass-

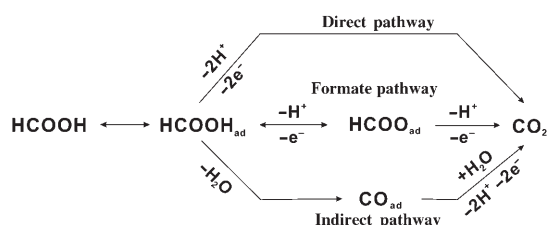


Figure 4. Tentative reaction scheme for the oxidation of formic acid on Pt which includes three different reaction pathways: the “indirect” pathway, the “formate pathway”, and the “direct” pathway. The formate pathway relates to the formate species detected by IR (see text).

transport conditions, and 2) demonstrated the potential of this setup for studies of electrocatalytic reactions by measurements of the electrooxidation of formic acid on a Pt film electrode in acidic solution at constant potentials between 0.4 and 0.6 V. These measurements allowed us to quantify the contributions of the different pathways proposed previously and to provide clear proof that under the present reaction conditions both pathways are minor. Direct oxidation of weakly adsorbed HCOOH_{ad} species to CO_2 is proposed to be the dominant reaction pathway.

Experimental Section

The electrolyte solutions were prepared by using p.a. grade formic acid, suprapure H_2SO_4 (Merck), and Millipore water (18.2 M Ω). They were de-aerated with highly pure Ar gas (6.0) for 20 min before each experiment. The Pt working electrode (exposed area $\approx 1 \text{ cm}^2$, surface roughness factor ≈ 10) was prepared by electroless Pt deposition on the Si prism, by following a procedure described in reference [10]; a Pt foil and a reversible hydrogen electrode (RHE) served as counter- and reference electrodes. All experiments were performed at room temperature. IR spectra were measured on a BioRad FTIR-6000 spectrometer equipped with a MCT detector (4-cm $^{-1}$ resolution, coaddition of five interferograms for each spectrum ($\approx 1 \text{ s}$ per spectrum)). The intensities are given by the absorbance, defined by $\log(R_0/R)$, where R_0 and R are the reflectance at the reference and sample potential, respectively. For background subtraction we used a spectrum recorded at the same potential in pure base electrolyte. This data processing results in spectra in which peaks pointing up reflect an increased absorption and peaks pointing down a loss of absorption.

Received: June 21, 2005

Revised: September 27, 2005

Published online: December 22, 2005

Keywords: electrochemistry · flow cell · IR spectroscopy · spectroelectrochemistry · time-resolved spectroscopy

- [1] B. Beden, J. M. Leger, C. Lamy, *Modern Aspects of Electrochemistry* (Eds.: B. Beden, J. M. Leger, C. Lamy, J. O. Bockris, B. E. Conway, R. E. White), Plenum, New York, **1992**, p. 97.
- [2] T. Iwasita, F. C. Nart, *Prog. Surf. Sci.* **1997**, *55*, 271–340, and references therein.
- [3] S.-G. Sun in *Electrocatalysis* (Eds.: J. Lipkowski, P. N. Ross), Wiley-VCH, New York, **1998**, pp. 243–290.
- [4] N. J. Harrick, *Internal Reflection Spectroscopy*, Harrick Scientific Products, Ossining, **1967**.
- [5] M. Osawa, *Handbook of Vibrational Spectroscopy*, Wiley, Chichester, **2002**, pp. 785–799.

- [6] W.-F. Lin, J.-T. Wang, R. F. Savinell, *J. Electrochem. Soc.* **1997**, *144*, 1917–1922.
- [7] C. Rice, S. Ha, R. I. Masel, A. Wieckowski, *J. Power Sources* **2003**, *115*, 229–235.
- [8] A. Capon, R. Parsons, *J. Electroanal. Chem.* **1973**, *45*, 205–231.
- [9] O. Wolter, J. Willsau, J. Heitbaum, *J. Electrochem. Soc.* **1985**, *132*, 1635–1638.
- [10] A. Miki, S. Ye, M. Osawa, *Chem. Commun.* **2002**, 1500–1502.
- [11] Z. Jusys, H. Massong, H. Baltruschat, *J. Electrochem. Soc.* **1999**, *146*, 1093–1098.
- [12] Z. Jusys, J. Kaiser, R. J. Behm, *Phys. Chem. Chem. Phys.* **2001**, *3*, 4650–4660.
- [13] M. R. Columbia, A. M. Crabtree, P. A. Thiel, *J. Am. Chem. Soc.* **1992**, *114*, 1231–1237.
- [14] S. C. Chang, M. J. Weaver, *J. Chem. Phys.* **1990**, *92*, 4582–4594.